

Polyaniline/nickel Composite Film Modified Electrode for Sensitive Electrochemical Determination of Ascorbic Acid

Mani Govindasamy¹, Veerappan Mani¹, Shen-Ming Chen^{1,}, Anandaraj Sathiyam², Johnson Princy Merlin², Gopal Boopathy³,*

¹ Department of Chemical Engineering and Biotechnology, National Taipei University of Technology, Taipei, Taiwan (ROC)

² Department of Chemistry, Bishop Heber College (Autonomous), Tiruchirappalli-620 017, Tamil Nadu, India

³ Department of Chemistry, College of Engineering, Guindy Campus, Anna University, Chennai 600 025

*Email: smchen78@ms15.hinet.net

Received: 24 September 2016 / Accepted: 27 October 2016 / Published: 10 November 2016

We have designed and fabricated a low-cost modified electrode based on polyaniline and Ni composite (PANI–Ni) for the sensitive determination ascorbic acid (AA). The composite formation was characterized by scanning electron microscopy, Energy-dispersive X-ray spectroscopy, electrochemical impedance spectroscopy and electrochemical methods. The PANI–Ni composite was used to modify the screen printed carbon electrode (SPCE) and the resulting modified electrode was used to develop AA sensor. The modified electrode shows excellent electrocatalytic activity to the oxidation of AA. An amperometric sensor was developed using PANI–Ni composite which delivered sensitive and prompt signals for AA. The linear range is 2–1210 μM , detection limit is 0.4 μM , and sensitivity is 0.479 $\mu\text{A}\mu\text{M}^{-1}\text{cm}^{-2}$. Moreover, the electrode has good repeatability, reproducibility and stability. The practical applicability of the electrode is demonstrated in human urine samples.

Keywords: Vitamin, antioxidants, biochemistry, conducting polymers, metals, electrocatalysis, electrochemical sensors

1. INTRODUCTION

Ascorbic acid (AA), is a vital nutrient for humans and it is extensively used in food industry [1, 2]. Among animal organs, the liver, leukocytes and anterior pituitary lobe show the highest concentrations of AA [3, 4]. It is involved in several biological roles including injuries healing, and in the synthesis of collagen, bones, blood vessels, and tendons [5, 6]. AA is also present in mammalian

brain along with several neurotransmitter amines [5, 7, 8]. It has been employed in the prevention and treatment of common cold, mental illness, infertility and cancer [3, 9, 10]. Due to the aforementioned importance of AA, its sensitive determination is highly important in clinical diagnosis from the point-of-care perception [5, 11]. The electrochemical methods are most preferable in the determination of AA, because they are simple, fast, low-cost, and portable [12, 13]. Unmodified electrodes are poor in selectivity, and reproducibility [14, 15] and hence properly designed chemical modifiers are necessary [3, 16]. These chemical modifiers are able to improve the selectivity, sensitivity and overall sensor performance [17, 18]. Notably, dopamine (DA) and uric acid (UA) are common interferences in AA sensing since their voltammetric signals are close to AA [11, 19-21]. Therefore, several modifiers are developed to separate their voltammetric peaks and simultaneous determination platforms are demonstrated. Besides, selective AA determination platform is also developed based on the different types of interactions (electrostatic and π stacking) between analytes (AA, DA and UA) and electrode surface [22, 23]. Some of the recently developed electrochemical AA sensors includes, nitrogen doped graphene [24], pristine graphene [17], exfoliated graphite paper [25], electrochemically reduced graphene oxide [26], and Pd nanoparticles/graphene oxide [5], protein-modified Au nanoclusters [27], conducting polymers [28] and DMF-exfoliated graphene [29] and ultrathin Pd nanowire [30] etc.,

Polyaniline (PANI) is well-known conducting polymer for its excellent electrocatalytic ability, conductivity and thermal stability [31-33]. Similarly, nickel nanoparticles (Ni) have good electrocatalytic properties, large surface area and good conductivity [34, 35]. In recent times, the composites prepared from conducting polymer and metal nanoparticles have found widespread electrochemical applicability [36, 37]. In the present work, we have prepared PANI/Ni composite via simple wet chemical method and developed a sensitive and selective sensor for the determination of AA. The composite is prepared through a simple wet chemical approach using cheaper precursors.

2. EXPERIMENTAL

2.1 Chemicals and Apparatus

Aniline, nickel chloride and all other reagents were purchased from Sigma-Aldrich and used as received. Double distilled water was used for all the experiments. 0.1 M phosphate buffer (pH 7.0) was prepared from sodium dihydrogen phosphate and disodium hydrogen phosphate and used as supporting electrolyte. Electrochemical studies were performed in a conventional three electrode cell using modified SPCE as a working electrode (area 0.3 cm^2), saturated Ag|AgCl (saturated KCl) as a reference electrode and Pt wire as a counter electrode. All the electrochemical measurements were carried out using CHI 1205a electrochemical work station (CH Instruments, Inc., U.S.A) at ambient temperature. Surface morphological studies were carried out using Hitachi S-3000 H scanning electron microscope (SEM). Energy-dispersive X-ray (EDX) spectra was recorded using Horiba Emax x-act (sensor + 24 V=16 W, resolution at 5.9 keV = 129 eV). EIM6ex Zahner (Kronach, Germany) was used for electrochemical impedance spectroscopy (EIS) studies.

2.2 Preparation of PANI–Ni/SPCE

First, 2 mM CTAB solution (10 mL) was prepared in 0.1 M H₂SO₄. Next, 30 mM aniline solution was added and the resulting solution was stirred for 20 min. The beaker was transferred to an ice-bath and the temperature was maintained below 0°C. Subsequently, 30 mL solution of 25 mM NiCl₂·6H₂O was added dropwise and stirred for 30 min. Afterwards, a pre-cooled solution of 50 mM ammonium peroxydisulfate was added in dropwise and continued stirring for another 30 min. The obtained precipitate was filtered and washed several times with water and acetone, respectively. The purified PANI/Ni composite was dried and redispersed (0.5 mg mL⁻¹) in water/ethanol (50/50; v/v) mixture. Next, 5 µL dispersion of PANI–Ni was dropped at the SPCE surface and dried at ambient conditions. The resulting PANI–Ni composite is used for further electrochemical studies.

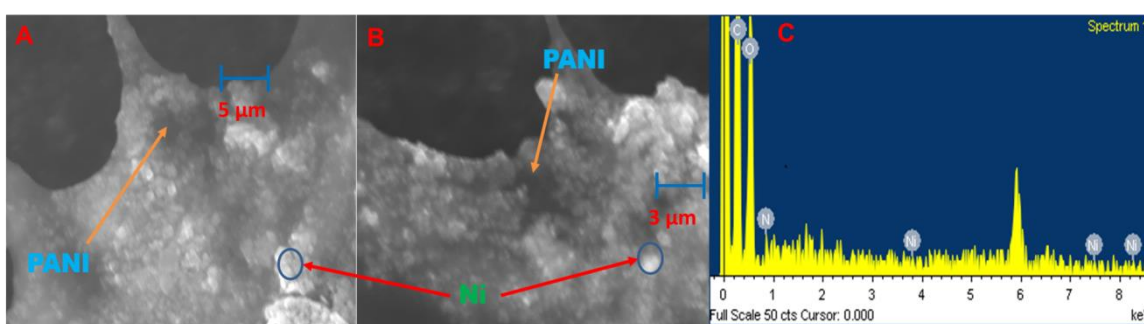


Figure 1. SEM images of PANI–Ni composite (A and B). EDX spectrum of PANI–Ni composite

3. RESULTS AND DISCUSSION

3.1 Characterization of PANI–Ni composite

The SEM images of PANI–Ni composite displays Ni particles decorated roughed surface of PANI layers (Figure 1A, B). Besides, the composite has good porous structure and abundant catalytic sites and the morphological results are consistent with previous reports [38–40]. Figure 1C displays the corresponding EDX profile of PANI–Ni composite which clearly showed signals for C, O and Ni atoms. The presence of Ni signal reveals the successful formation of composite. Figure 2 displays the Electrochemical impedance spectroscopy (EIS) is an efficient tool to examine the electrochemical properties and interfacial changes of the modified electrodes [41]. EIS curves obtained at unmodified SPCE (a), Ni/SPCE (b), PANI/SPCE (c) and PANI–Ni/SPCE (d) in 0.1 M KCl containing 5 mM Fe(CN)₆^{3-/4-}. The diameters of the semicircle portion of the curves are in the following order: bare SPCE > Ni/SPCE > PANI/SPCE > PANI–Ni/SPCE. The charge transfer resistance (R_{ct}) values of bare SPCE, Ni/SPCE, PANI/SPCE and PANI–Ni/SPCE are 432, 206, 102 and 53 Ω, respectively. The R_{ct} value obtained at PANI–Ni/SPCE is the smallest among the control electrodes which clearly revealed that the prepared composite has very less resistance. In other words, the PANI–Ni/SPCE has higher electrical conductivity over other electrodes and this behaviour of the composite is useful for the development of sensitive sensors [42].

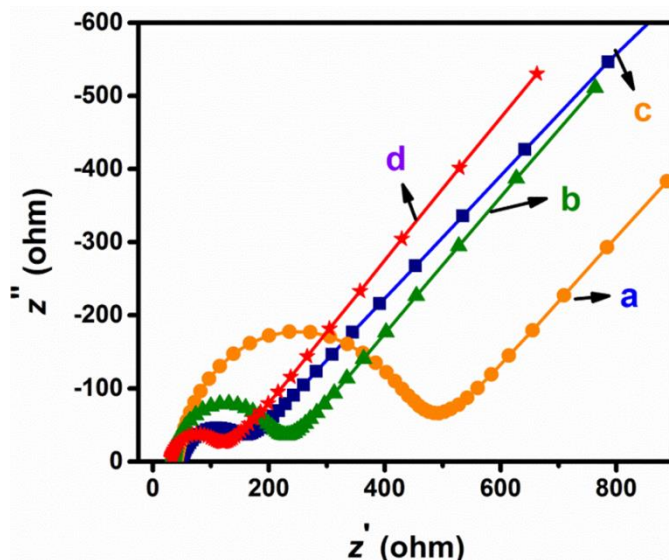


Figure 2. EIS curves of bare SPCE (a), Ni/SPCE (b), PANI/SPCE (c), and PANI-Ni/SPCE (d)

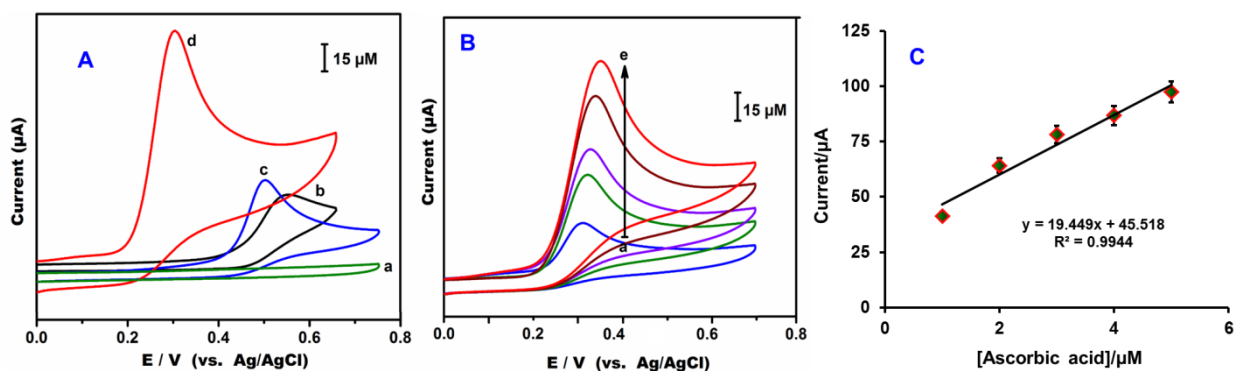


Figure 3. (A) CVs obtained at bare SPCE (a), PANI/SPCE (b), Ni/SPCE (c) and PANI-Ni/SPCE (d) in phosphate buffer (pH 7.0) containing 5 μM AA. Scan rate = 50 mV s⁻¹. (B) CVs obtained at PANI-Ni/SPCE in phosphate buffer (pH 7.0) containing different concentrations of AA (1 to 10 μM). (C) Plot between [AA] (μM) vs. response current (μA).

3.2 Electrochemical oxidation of AA at PANI-Ni/SPCE

Figure 3A shows the cyclic voltammograms (CVs) obtained at bare SPCE (a), PANI/SPCE (b), Ni/SPCE (c) and PANI-Ni/SPCE (d) in phosphate buffer (pH 7.0) containing 5 μM AA. The scan rate is 50 mV s⁻¹. The unmodified SPCE displays poor electrocatalytic ability to oxidize AA. Compared with unmodified electrode, PANI/SPCE and Ni/SPCE have shown better electrocatalytic to AA; however the oxidation occurred at higher overpotential which will leads to high level of interference. On the other hand, PANI-Ni/SPCE has shown excellent electrocatalytic ability to oxidize AA at lesser overpotential (0.28 V) and sharp peak with enhanced peak current. The location of AA oxidation peak at PANI-Ni/SPCE is 0.32 V which is about 170 mV and 230 mV lower potential than Ni/SPCE and PANI/SPCE, respectively. Besides, the composite owns large surface area, high

conductivity and abundant catalytic sites and these characteristics of the composite favored the obtained high electrocatalytic ability of the composite [43]. Previous studies revealed that the composites of conducting polymers and metal particles possess good synergic effect between them which greatly accelerates their electrocatalysis [44, 45]. Our studies also revealing that PANI–Ni composite has synergic effect towards electrocatalysis of AA consistent with previous results [46, 47].

Figure 3B shows the CV curves obtained at PANI–Ni/SPCE in phosphate buffer (pH 7) containing different concentrations of AA. The oxidation peak current increases linearly as the concentrations of AA increases. The linear increment in peak current indicates the electrode surface is not damaged by electrode fouling. The plot between concentrations of AA and their corresponding response currents exhibits good linearity with slope of $19.45 \mu\text{A}/\mu\text{M}$ (Figure 3C). The influence of different scan rates towards the electrocatalysis reaction of AA at PANI–Ni/SPCE is studied (Figure 4A). The anodic peak of AA is increased linearly as the scan rate increases from 50 to 500 mVs^{-1} . The plot between anodic peak current and scan rates showed good linearity which indicating that the oxidation process is a surface controlled diffusion process (Figure 4B) and this result is consistent with previous reports [48].

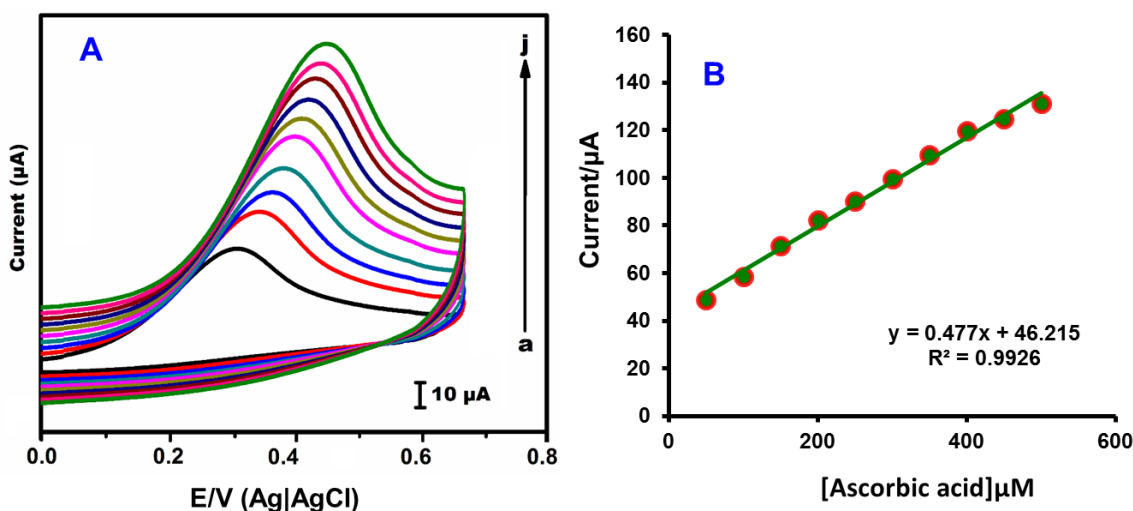


Figure 4. (A) Cyclic voltammograms of PANI–Ni/SPCE towards $5 \mu\text{M}$ AA at different scan rates from 50 to 500 mV s^{-1} (a=50, b=100, c=150, d=200, e=250, f=300, g=350, h=400, i=450 and j=500 mV s^{-1}). (B) Anodic peak current (μA) vs. scan rate (mV s^{-1})

3.4 Determination of AA

Figure 5A displays the amperometric responses of PANI–Ni/SPCE towards sequential additions of AA into phosphate buffer (pH 7). The applied potential was $+0.28 \text{ V}$ and rotation speed was 1200 RPM. For each addition, a sharp rise in the response current is observed and 95% of steady-state current is reached within 5s. Thus, the PANI–Ni composite film delivered prompt and sensitive responses to AA. The amperometric response current increased linearly on further AA injections. The linear increase in the oxidation peak current shows the great electrocatalytic ability of the fabricated modified electrode. The concentration dependent linear plot showed excellent linearity with slope of

0.1437 $\mu\text{A } \mu\text{M}^{-1}$ (Figure 5B). The response was linear in wide concentration range of 2–1210 μM with sensitivity of 0.479 $\mu\text{A}\mu\text{M}^{-1} \text{cm}^{-2}$. The limit of detection (LOD) is calculated to be 0.62 μM . The LOD was calculated using the formula, $\text{LOD} = 3 s_b/S$ where, s_b is the standard deviation of ten blank measurements and S is the sensitivity [15]. The important parameters of sensor, such as LOD and linear range were compared with previously modified electrodes [17, 19, 23, 30, 49–54] and given as **Table 1**. As can be seen from the table, our electrode exhibits either higher or comparable sensor performance over previously reported electrodes. Compared with the cost of previously reported several graphene and carbon nanotubes based composites [52–54], the cost required to prepare PANI–Ni composite is very less. In addition, the preparation of the PANI–Ni composite involves easy steps and does not require any hazardous materials. Thus, our studies revealed that the PANI–Ni composite incorporated modified electrode has good potential in the development of robust AA sensor.

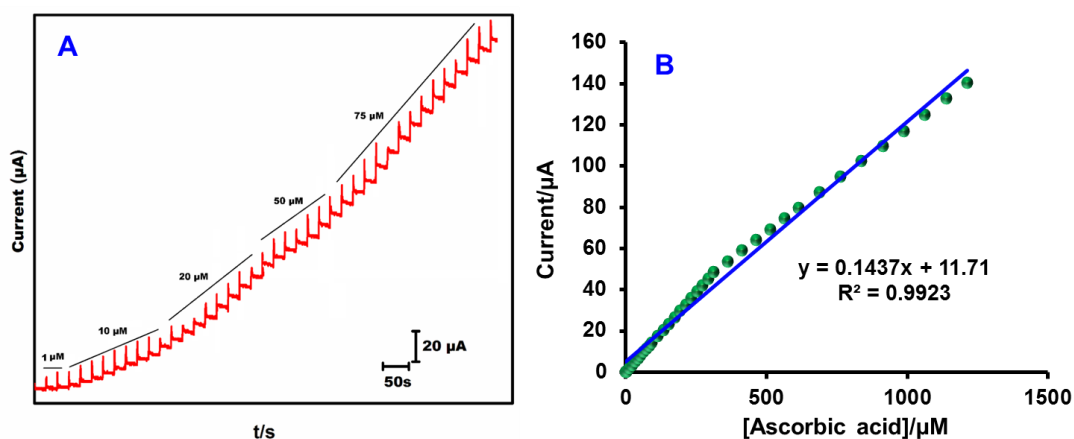


Figure 5. (A) Amperometric response obtained at PANI–Ni composite film modified electrode towards each sequential additions of AA into continuously stirred phosphate buffer (pH 7). The rotation speed = 1500 RPM and electrode potential = + 0.28 V. (B) [AA]/ μM vs. response current (μA).

Table 1. Comparison of the performance of PANI–Ni composite film based AA sensor with previously reported chemical modifiers

Electrodes	Linear range/ μM	Detection limit/ μM	Ref.
Pristine graphene	9.00–2314	6.45	[17]
Graphene/Pt nanocomposite	0.15–34.4	0.15	[19]
Carbon supported NiCoO ₂ nanoparticles	10–2630	0.5	[23]
Ultrathin Pd nanowire	25–900	0.2	[30]
Graphene/Pd–Pt nanoparticles	40–1200	0.61	[49]
N-doped carbon nanotubes/Fe ₃ O ₄ nanoparticles	5–235	0.24	[50]
Carbon supported PdNi nanoparticles	10–1800	0.5	[51]
Amino-group functionalized mesoporous Fe ₃ O ₄ @Graphene	5–1600	0.074	[52]
Carbon nanotubes/mesocellular graphene foam	100–6000	18.28	[53]
Reduced graphene oxide/Au nanoplates	240–1500	51	[54]
PANI–Ni	2–1210	0.62	This work

3.5 Real sample analysis

Next, we have tested the practical feasibility of the fabricated modified electrode towards determination of AA present in spiked human urine sample. The sample was collected from a healthy man. About 2 mL of human urine sample was diluted with 50 mL phosphate buffer (pH 7) and known concentrations of AA were spiked into the solution. Amperometric experiments were carried out using this solution and the PANI–Ni composite film modified electrode delivers quick and sensitive amperometric signals. The added, found and recovery values were calculated and given as Table 2. It can be seen from the table that the electrode detects AA in real samples with satisfactory range of recoveries [55]. Thus, the fabricated modified electrode has great potential for real time AA detection in clinical samples.

Table 2. Determination of AA in real samples using PANI–Ni composite

Real sample	Added/ μM	Found/ μM	Recovery/%	*RSD/%
Human urine sample	5	4.89	97.8	4.11
	10	9.72	97.2	3.94

* Related standard deviation (RSD) of 3 independent experiments

3.6 Repeatability, reproducibility and stability

Repeatability of the electrode was evaluated by performing six repetitive measurements using individually prepared PANI–Ni composite film modified electrodes. The sensor performance of the electrodes were studied towards 10 μM AA. The PANI–Ni composite exhibits satisfactory repeatability with RSD of 3.945%. Similarly, reproducibility of the electrode had been tested for five independent measurements which were carried out using five modified electrodes. The electrode exhibits acceptable reproducibility with RSD of 4.05% for the determination of AA. In order to determine storage stability of the electrode, its electrocatalytic response towards 10 μM AA was monitored every day. During 10 days storage period, about 92.26% of initial response currents of AA was retained indicates excellent storage stability. Thus, the fabricated electrode displayed good stability, reproducibility and repeatability which are comparable to the previous reports [56, 57].

4. CONCLUSIONS

In summary, a sensitive and highly selective electrochemical AA detection platform was developed using PANI–Ni composite. The successful formation of the composite was confirmed by SEM, EDX, EIX and CV studies. The electrochemical studies proved that the composite has excellent electrocatalytic ability to the oxidation of AA. The composite showed less overpotential and high peak current for the oxidation of AA. The amperometric detection methods showed wide linear range of 2–

1210 μM . The sensitivity is $0.479 \mu\text{A}\mu\text{M}^{-1} \text{cm}^{-2}$ and the detection limit is $0.62 \mu\text{M}$. The other advantages of the sensor are its satisfactory stability, repeatability, reproducibility and potential practical applicability.

ACKNOWLEDGEMENTS

This work was supported by the Ministry of Science and Technology (MOST), Taiwan (ROC).

References

1. F. Li, J. Li, Y. Feng, L. Yang, Z. Du, *Sens. Actuators, B*, 157 (2011) 110.
2. Y. Song, C. Gong, D. Su, Y. Shen, Y. Song, L. Wang, *Anal. Methods*, 8 (2016) 2290.
3. S. Thiagarajan, S.-M. Chen, *Talanta*, 74 (2007) 212.
4. I. Gualandi, M. Marzocchi, E. Scavetta, M. Calienni, A. Bonfiglio, B. Fraboni, *J. Mat. Chem. B*, 3 (2015) 6753.
5. G.-h. Wu, Y.-f. Wu, X.-w. Liu, M.-c. Rong, X.-m. Chen, X. Chen, *Anal. Chim. Acta*, 745 (2012) 33.
6. J. Du, J.J. Cullen, G.R. Buettner, *Biochim Biophys Acta.*, 1826 (2012) 443.
7. Q. Lian, Z. He, Q. He, A. Luo, K. Yan, D. Zhang, X. Lu, X. Zhou, *Anal. Chim. Acta*, 823 (2014) 32.
8. M. Ganiga, J. Cyriac, *Anal. Bioanal. Chem.*, 408 (2016) 3699.
9. F. Li, C. Tang, S. Liu, G. Ma, *Electrochim. Acta*, 55 (2010) 838.
10. S. Gariballa, *Int J Vitam Nutr Res.* 84 (2014) 12.
11. D. Han, T. Han, C. Shan, A. Ivaska, L. Niu, *Electroanalysis*, 22 (2010) 2001.
12. J.-C. Chen, H.-H. Chung, C.-T. Hsu, D.-M. Tsai, A. Kumar, J.-M. Zen, *Sens. Actuators, B*, 110 (2005) 364.
13. M. Govindasamy, V. Mani, S.-M. Chen, R. Karthik, K. Manibalan, R. Umamaheswari, *Int. J. Electrochem. Sci.*, 11 (2016) 2954.
14. A.J. Bard, L.R. Faulkner, *Electrochemical methods: fundamentals and applications*, Wiley New York 1980.
15. V. Mani, A.P. Periasamy, S.-M. Chen, *Electrochem. Commun.*, 17 (2012) 75.
16. K. Rawat, A. Sharma, P.R. Solanki, H. Bohidar, *Electroanalysis*, 27 (2015) 2448.
17. S. Qi, B. Zhao, H. Tang, X. Jiang, *Electrochim. Acta*, 161 (2015) 395.
18. J. Lavanya, N. Gomathi, *Talanta*, 144 (2015) 655.
19. C.-L. Sun, H.-H. Lee, J.-M. Yang, C.-C. Wu, *Biosens. Bioelectron.*, 26 (2011) 3450.
20. J. Ping, J. Wu, Y. Wang, Y. Ying, *Biosens. Bioelectron.*, 34 (2012) 70.
21. V.K. Ponnusamy, V. Mani, S.-M. Chen, W.-T. Huang, J. Jen, *Talanta*, 120 (2014) 148.
22. J. Du, R. Yue, Z. Yao, F. Jiang, Y. Du, P. Yang, C. Wang, *Colloids Surf., A*, 419 (2013) 94.
23. X. Zhang, S. Yu, W. He, H. Uyama, Q. Xie, L. Zhang, F. Yang, *Biosens. Bioelectron.*, 55 (2014) 446.
24. Z.-H. Sheng, X.-Q. Zheng, J.-Y. Xu, W.-J. Bao, F.-B. Wang, X.-H. Xia, *Biosens. Bioelectron.*, 34 (2012) 125.
25. W. Cai, T. Lai, H. Du, J. Ye, *Sens. Actuators, B*, 193 (2014) 492.
26. L. Yang, D. Liu, J. Huang, T. You, *Sens. Actuators, B*, 193 (2014) 166.
27. X. Wang, P. Wu, X. Hou, Y. Lv, *Analyst*, 138 (2013) 229.
28. A. Ambrosi, A. Morrin, M.R. Smyth, A.J. Killard, *Anal. Chimi. Acta*, 609 (2008) 37.
29. G.P. Keeley, A. O'Neill, N. McEvoy, N. Peltekis, J.N. Coleman, G.S. Duesberg, *J. Mater. Chem.*, 20 (2010) 7864.
30. D. Wen, S. Guo, S. Dong, E. Wang, *Biosens. Bioelectron.*, 26 (2010) 1056.

31. S. Khalili, B. Khoshandam, M. Jahanshahi, *RSC Adv.*, 6 (2016) 35692.
32. B.J. Gallon, R.W. Kojima, R.B. Kaner, P.L. Diaconescu, *Angew. Chem. Int. Ed.*, 46 (2007) 7251.
33. W. Zhou, Y. Yu, H. Chen, F.J. DiSalvo, H.c.D. Abruña, *J. Am. Chem. Soc.*, 135 (2013) 16736.
34. K.-C. Lin, Y.-C. Lin, S.-M. Chen, *Electrochim. Acta*, 96 (2013) 164.
35. P.Z. Li, A. Aijaz, Q. Xu, *Angew. Chem. Int. Ed.*, 51 (2012) 6753.
36. M. Tumma, R. Srivastava, *Catal. Commun.*, 37 (2013) 64.
37. D. Zhai, B. Liu, Y. Shi, L. Pan, Y. Wang, W. Li, R. Zhang, G. Yu, *ACS nano*, 7 (2013) 3540.
38. A. Batool, F. Kanwal, S. Riaz, A. Abbas, S. Naseem *Mater. Today: Proc.*, 2 (2015) 5201.
39. L. Gu, X. Zhao, X. Tong, J. Ma, B. Chen, S. Liu, H. Zhao, H. Yu, J. Chen, *Int. J. Electrochem. ci.*, 11 (2016) 1621.
40. A.Y. Obaid, E.H. El-Mossalamy, S.A. Al-Thabaiti, I.S. El-Hallag, A.A. Hermas, A.M. Asiri, *Int. J. Electrochem. Sci.*, 9 (2014) 1003.
41. V. Mani, A.T.E. Vilian, S.-M. Chen, *Int. J. Electrochem. Sci.*, 7 (2012) 12774.
42. A.S. Sarac, M. Ates, B. Kilic, *Int. J. Electrochem. Sci.*, 3 (2008) 777.
43. Rajesh, T. Ahuja, D. Kumar, *Sens. Actuators, B*, 136 (2009) 275.
44. S.J. Park, O.S. Kwon, J.E. Lee, J. Jang, H. Yoon, *Sensors* 14 (2014) 3604.
45. Q. Xu, J. Leng, H.-b. Li, G.-j. Lu, Y. Wang, X.-Y. Hu, *React. Funct. Polym.*, 70 (2010) 663.
46. S. Tian, J. Liu, T. Zhu, W. Knoll, *Chem. Mater.*, 16 (2004) 4103.
47. J.M. Kinyanjui, N.R. Wijeratne, J. Hanks, D.W. Hatchett, *Electrochim. Acta* 51 (2006) 2825
48. M. Govindasamy, V. Mani, S.-M. Chen, A. Sathiyar, J.P. Merlin, V.K. Ponnusamy, *Int. J. Electrochem. Sci.*, 11 (2016) 8730.
49. J. Yan, S. Liu, Z. Zhang, G. He, P. Zhou, H. Liang, L. Tian, X. Zhou, H. Jiang, *Colloids Surf., B*, 111 (2013) 392.
50. D.M. Fernandes, M. Costa, C. Pereira, B. Bachiller-Baeza, I. Rodríguez-Ramos, A. Guerrero-Ruiz, C. Freire, *J. colloid interface Sci.*, 432 (2014) 207.
51. X. Zhang, Y. Cao, S. Yu, F. Yang, P. Xi, *Biosens. Bioelectron.*, 44 (2013) 183.
52. D. Wu, Y. Li, Y. Zhang, P. Wang, Q. Wei, B. Du, *Electrochim. Acta*, 116 (2014) 244.
53. H. Li, Y. Wang, D. Ye, J. Luo, B. Su, S. Zhang, J. Kong, *Talanta*, 127 (2014) 255.
54. C. Wang, J. Du, H. Wang, C.e. Zou, F. Jiang, P. Yang, Y. Du, *Sens. Actuators, B*, 204 (2014) 302.
55. K.S. Ngai, W.T. Tan, Z. Zainal, R.M. Zawawi, M. Zidan, *Int. J. Electrochem. Sci.*, 8 (2013) 10557.
56. J. Zhang, Z. Zhu, J. Zhu, K. Li, S. Hua, *Int. J. Electrochem. Sci.*, 9 (2014) 1264.
57. M. Arvand, S. Sohrabnezhad, M.F. Mousav, M. Shamsipur, M.A. Zanjanchi, *Anal. Chim. Acta*, 491 (2003) 193.